Topography and Radiation Exchange of a Mountainous Watershed

HAILIANG FU AND STANISLAW J. TAJCHMAN

Division of Forestry, West Virginia University, Morgantown, West Virginia

JAMES N. KOCHENDERFER

Northeastern Forest Experiment Station, Parsons, West Virginia

(Manuscript received 2 March 1994, in final form 21 July 1994)

ABSTRACT

This report deals with the radiation exchange of a complex terrain. A relatively simple network for computing topographic parameters, global radiation, and net radiation of a mountainous terrain was developed and applied to a forested Appalachian watershed encompassing 39.2 ha (Watershed 4, U.S. Forest Service at Parsons, West Virginia, 39°20'N, 79°40'W). Monthly sums of global radiation and net radiation of the watershed were computed for the period of 40 years (1951–90). Topographic map of the watershed in scale 1:2500 and data on global radiation at a horizontal surface in the study area (1955–77), monthly average air temperature, moisture, and cloudiness were used in the analysis.

The topographic analysis showed that for the 432 terrain segments, covering the whole area of the watershed, the average daily possible sunshine duration varied from 9.3 to 11.9 h, with an average of 11.0 h, which is about 92% of the possible sunshine duration at a horizontal surface at the study area. The sky view factor VF (i.e., that fraction of the sky that can be seen from the center of gravity of a terrain segment) was obtained for all terrain segments and applied in computing their diffuse radiation. The average value of VF of the watershed was 0.91, ranging from 0.65 to 0.98. The conversion factor for direct radiation R_b (i.e., the ratio of direct radiation flux at a slope to that at a horizontal plane in absence of the atmosphere) in the watershed varied from 0.39 to 1.41 (average 1.11). The seasonal variations of sunshine duration and conversion factor at slopes with different azimuths were also analyzed.

The prediction of radiation exchange showed that for the watershed, the average yearly sums of global radiation and net radiation were about 4.5 and 2.2 GJ m^{-2} yr^{-1}, respectively. On the yearly average, the upper east-facing slopes received 20%–30% more direct radiation than a horizontal surface, but the north-facing slopes and the lower sites in the watershed received 10%–20% less.

The seasonal changes of R_b values at slopes with different azimuths in the watershed were described. The relationships between solar movement and average values of R_b, shortwave radiation absorbed, and net radiation at different segment groups were developed.

The estimated relative errors of predicted global radiation and net radiation in the watershed were within about 10% for the average yearly sums.

1. Introduction

The knowledge of solar radiation income and net radiation is important in landscape ecology, in studies of the energy balance of plant communities, and it has technological applications such as renewable energy conversion and climate change research. Solar radiation reaching the earth's surface is composed of direct radiation and diffuse radiation. While flux density of direct radiation varies with the angle of incidence, the diffuse radiation is often accepted to be isotropic (e.g., Liu and Jordan 1962). Radiation data are, as a rule, available for a horizontal surface with unrestricted horizon, and they can not be applied directly to a complex terrain where both components of global radiation are modified by topographic parameters such as slope azimuth and inclination and restriction of the horizon.

There is abundant literature on computing solar radiation income on inclined surfaces, for example, the studies by Liu and Jordan (1962), Klein (1977, 1981), Kondratyev (1977), and Perez and Stewart (1984). Klein (1977, 1981) gave relationships for calculating global radiation on arbitrarily oriented surfaces. However, his relationships do not account for the effects of surrounding terrain. In the approach suggested by Tajchman (1975), the relationships between solar radiation income and parameters of terrain can be described in one coordinate system.

In this paper, based on the previous studies by Tajchman (1975), Klein (1981), and Erbs et al. (1982), the relationships for computing monthly sums of global radiation and net radiation for a forested wa-

Corresponding author address: Dr. Stanislaw J. Tajchman, Division of Forestry, West Virginia University, P.O. Box 6125, Morgantown, WV 26506-6125.

tershed were developed using global radiation data for a horizontal surface in the study area and climatological data on air temperature, moisture, and cloudiness (Fu 1992).

2. Topographic analysis

Global radiation data for a horizontal surface can be used for computing corresponding values for a complex terrain if specific parameters are known. They include slope azimuth and inclination, sky view factor, and the conversion factor for direct radiation, which is equal to the ratio of the direct radiation incident upon the sloped surface during a day to the direct radiation on a horizontal surface during the same period (Iqbal 1983). To obtain these parameters the complex terrain is considered in the X, Y, Z coordinate system. The terrain area is divided into triangular segments, which are approximated to elements of planes. The size of the triangles depends on the spatial variability of topography; that is, with increasing complexity of the terrain, the average area of triangles will decrease (Tajchman 1975).

Theoretical procedures will be demonstrated in developing the topographic analysis of Watershed 4 at the U.S. Forest Service, Fernow Experimental Forest near Parsons, West Virginia. The watershed area is 39.2 ha and the elevation ranges from 739 to 869 m. It has a southeast orientation, and the average slope inclination is 14°. This watershed has been a subject of hydrological and forest ecological studies for more than 40 years, and this paper is to assist current research in progress.

The topographic analysis was based on the map of the watershed in a scale of 1:2500, considered in the coordinate system with X axis directed to the east, Y axis directed to the north, and Z axis directed to zenith. The triangulated network originally proposed by Tajchman (1975), which is essentially the same as the triangulated irregular network (TIN) reported by Peuker et al. (1978) [cited by Burrough (1986)], was used to digitize the study area. A TIN can avoid the redundancies of the regular rectangular or octagonal grid systems commonly used in the geographic information system (GIS) and can specifically follow ridges, streamlines, and other topological features that can be digitized to the accuracy required (Burrough 1986). The watershed was divided into 432 triangular segments with an average area of 360 m^2. The triangles were formed between contour lines with an elevation difference of about 15 m (Fig. 1) using a Summagraphics Microgrid II digitizer (Summagraphics Corp., Fairfield, Connecticut,).

The equation of a plane determined by three points, $P_1(X_1, Y_1, Z_1)$, $P_2(X_2, Y_2, Z_2)$, and $P_3(X_3, Y_3, Z_3)$ is given by

$$Ax + By + Cz + D = 0, \tag{1}$$

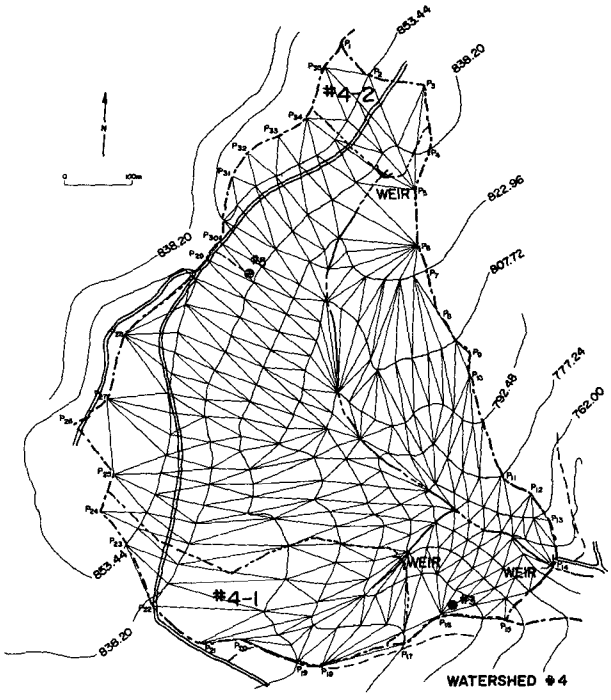

FIG. 1. Topography and triangulated network of Watershed 4. Contour lines represent the elevation (m).

where

$$A = (Y_2 - Y_1)(Z_3 - Z_1) - (Y_3 - Y_1)(Z_2 - Z_1),$$
$$B = (Z_2 - Z_1)(X_3 - X_1) - (X_2 - X_1)(Z_3 - Z_1),$$
$$C = (X_2 - X_1)(Y_3 - Y_1) - (Y_2 - Y_1)(X_3 - X_1),$$
$$D = -(AX_1 + BY_1 + CZ_1). \tag{2}$$

The area S of a triangle can be calculated as follows:

$$S = \frac{1}{2}|(Y_3 - Y_1)(Z_3 - Z_2) + (X_3 - X_2)(Z_3 - Z_1) + (X_3 - X_1)(Y_3 - Y_2) - (X_3 - X_2)(Y_3 - Y_1) - (Y_3 - Y_2)(Z_3 - Z_1) - (Z_3 - Z_2)(X_3 - X_1)|. \tag{3}$$

The inclination β of the plane is given by

$$\cos\beta = \pm C(A^2 + B^2 + C^2)^{-1/2}. \tag{4}$$

The azimuth α of the plane is 0° due north, and it increases clockwise over east (90°), south (180°), and west (270°). It can be calculated in the following steps:

First, substituting $Z = 0$ in Eq. (1), we obtain

$$Ax + By + D = 0. \tag{5}$$

This equation describes the line of intersection of the plane [Eq. (1)] with the horizontal plane ($Z = 0$). The

line normal to the line of intersection and passing through the origin of the coordinate system is given by

$$y = \frac{B}{A}x. \tag{6}$$

This line has the same direction as the azimuth of the terrain segment under consideration. The angle α' between the line [Eq. (6)] and X axis can be obtained from the following relationship:

$$\alpha' = \arctan\left(\frac{B}{A}\right). \tag{7}$$

Second, express Eq. (1) in the normal form:

$$UX + VY + WZ = 1, \tag{8}$$

where $U = -A/D$, $V = -B/D$, and $W = -C/D$.

Finally, the azimuth α can be calculated according to the value of α' and the signs of U, V, and W (Table 1).

The sky view factor VF is defined as that fraction of the sky that can be seen from the center of gravity CG of a terrain segment. To compute VF, the ridgeline of the watershed was represented as a sequence of the segments of straight lines marked in Fig. 1 by the points $P_1, \ldots, P_{35}$. The origin of the coordinate system was placed at CG (x_c, y_c, z_c). The horizon restriction is determined by the sum of solid angles formed between the ridgeline segments and the horizontal plane passing through CG (Fig. 2). The projections of P_i on the horizontal plane are marked as $M_i(x_i, y_i, z_c)$. The following relationships were used to obtain the elevation angles γ_i, γ_{i+1}, and those between the corresponding vertical planes ϵ_i:

$$\tan\gamma_i = \frac{Z_i - Z_c}{[(x_i - x_c)^2 + (y_i - y_c)^2]^{1/2}}$$

$$\tan\gamma_{i+1} = \frac{Z_{i+1} - Z_c}{[(x_{i+1} - x_c)^2 + (y_{i+1} - y_c)^2]^{1/2}}$$

$$\epsilon_i = \left|\arctan\frac{y_{i+1} - y_c}{x_{i+1} - x_c} - \arctan\frac{y_i - y_c}{x_i - x_c}\right|. \tag{9}$$

TABLE 1. Signs of the parameters U, V, and W, and definition of the azimuth α of terrain segments.

Signs of coefficients			
U	V	W	Azimuth α
+	+	+	$90 - \alpha'$
−	−	−	$90 - \alpha'$
+	−	+	$90 + \alpha'$
−	+	−	$90 + \alpha'$
+	+	−	$270 - \alpha'$
−	−	+	$270 - \alpha'$
+	−	−	$270 + \alpha'$
−	+	+	$270 + \alpha'$

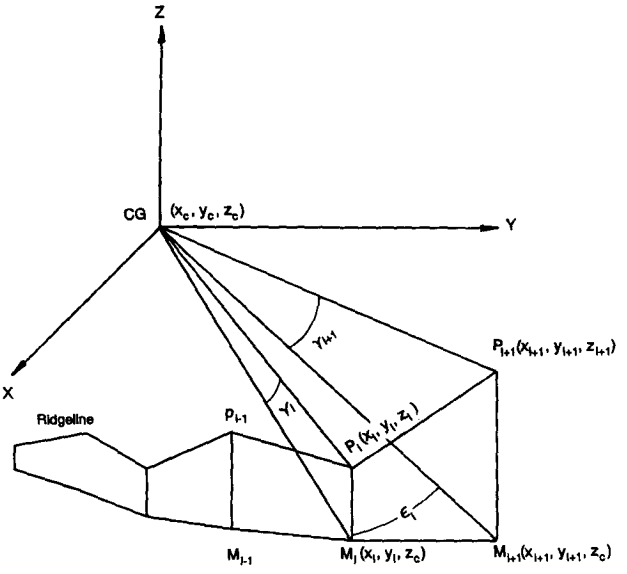

FIG. 2. Diagram for computing solid angle formed by a terrain segment above the horizontal plane.

The solid angle S_i, formed by γ_i, γ_{i+1}, and ϵ_i, is given by

$$S_i = \frac{\gamma_i + \gamma_{i+1}}{2}\epsilon_i \cos\left(\frac{\gamma_i + \gamma_{i+1}}{2}\right), \tag{10}$$

where γ_i, γ_{i+1}, and ϵ_i are in radians. The view factor of the ith terrain segment VF_i is given by

$$\mathrm{VF}_i = 1 - \frac{\sum S_i}{2\pi}, \tag{11}$$

where $\sum S_i$ is the sum of solid angles formed between the ridgeline and the horizontal plane passing through CG of the segment.

3. Possible sunshine duration and conversion factor

The possible sunshine duration S_D is the amount of time from sunrise to sunset. For an unobstructed horizontal plane, S_D can be obtained as

$$S_D = \frac{2\omega_s}{15}, \tag{12}$$

with $\omega_s = \cos^{-1}(-\tan\phi\,\tan\delta)$, where ω_s is the hour angle at sunset, ϕ is latitude of the site, and δ is solar declination. In the case of mountainous terrain, this formula is not applicable; and the horizon restriction on S_D must be taken into account.

The conversion factor for direct radiation R_b (i.e., the ratio of direct radiation flux at a slope to that at a horizontal surface in absence of the atmosphere) can be obtained as follows (Klein 1977, 1981):

$$R_b = \Big(\cos\beta \sin\delta \sin\phi\,|\omega_{ss} - \omega_{sr}|\,\frac{\pi}{180} - \sin\delta \cos\phi \sin\beta \cos\alpha\,|\omega_{ss} - \omega_{sr}|\,\frac{\pi}{180} + \cos\phi \cos\delta \cos\beta\,|\sin\omega_{ss} - \sin\omega_{sr}| + \cos\delta \cos\alpha \sin\phi \sin\beta\,|\sin\omega_{ss} - \sin\omega_{sr}| + \cos\delta \sin\beta \sin\alpha\,|\cos\omega_{ss} - \cos\omega_{sr}|\Big) \times \left\{2\left[\cos\phi \cos\delta \sin\omega_s + \left(\frac{\pi}{180}\right)\omega_s \sin\phi \sin\delta\right]\right\}^{-1}, \quad (13)$$

where β is slope inclination; δ is solar declination; ϕ is latitude; α is slope azimuth; ω_s is sunset hour angle for a horizontal surface; ω_{ss} and ω_{sr} are sunset and sunrise hour angles for the inclined surface, respectively.

Klein (1977, 1981) has developed an algorithm for computing ω_{ss} and ω_{st} for inclined planes. The effect of surrounding terrain on ω_{ss} and ω_{st} was considered by Tajchman (1975). For each terrain segment, the straight line between CG and the sun will intersect with the ridge line at a point $P(x, y, z)$ at least once at sunrise and at sunset. To determine the position of the points of intersection, the sun's elevation h was computed from the following equation (Iqbal 1983):

$$\sin h = \sin\delta \sin\phi + \cos\delta \cos\phi \cos\omega. \quad (14)$$

We computed the value of h for 10-min intervals from sunrise to sunset and compared it to the elevation of the ridgeline. When the sun moves from below to above the ridgeline (or from above to below), the point of sunrise (or sunset) is identified. The coordinates of this point, and the corresponding values of h and the azimuth of the sun A_s, can be obtained from the solution of the following equations:

$$\frac{x - x_i}{x_{i+1} - x_i} = \frac{y - y_i}{y_{i+1} - y_i} = \frac{z - z_i}{z_{i+1} - z_i},$$

$$y = x \tan A_s,$$

$$z = (X^2 + y^2)^{1/2} \tan h,$$

$$\cos A_s = \frac{\sin h \sin\phi - \sin\delta}{\cos h \cos\phi}, \quad (15)$$

where ϕ is latitude and δ is the sun's declination. The solution of the above equations yields the relationship

$$\sin^2 h + J \sin h + K = 0, \quad (16)$$

where

$$J = \frac{2(HI - \sin\phi \sin\delta)}{H^2 + 1},$$

$$K = \frac{\sin^2\delta + I^2 - \cos^2\phi}{H^2 + 1},$$

$$H = -\frac{b \sin\phi + c \cos\phi}{a},$$

$$I = \frac{b}{a}\sin\delta,$$

$$a = (x_{i+1} - x_i)z_i - (z_{i+1} - z_i)x_i,$$

$$b = (z_{i+1} - z_i)y_i - (y_{i+1} - y_i)z_i,$$

$$c = (y_{i+1} - y_i)x_i - (x_{i+1} - x_i)y_i. \quad (17)$$

The solution of Eq. (16) can be obtained as follows:

1) If $(b/a)^2 \leq (\cos\phi/\sin\delta)^2 - 1$, then

$$\sin h = \frac{(J^2 - 4K)^{1/2} - J}{2}; \quad (18)$$

2) If $(b/a)^2 > (\cos\phi/\sin\delta)^2 - 1$, two cases should be considered:

(a) If $J < -(J^2 - 4K)^{1/2}$, then

$$\sin h = \frac{-J \pm (J^2 - 4K)^{1/2}}{2}. \quad (19)$$

Only one solution of Eq. (19) satisfies $0 \leq h \leq h_0$, with $h_0 = 90° - \phi + \delta$. This solution yields the hour angle of the sun at sunrise (or sunset).

(b) If $J \geq (J^2 - 4K)^{1/2}$, then $h \leq 0$. This means that the point of intersection is at or below the horizontal surface passing through CG. The hour angle of sunset (or sunrise), in this case, will be the value of ω_s obtained in Eq. (12).

Substituting $\sin h$ from Eqs. (18) or (19) into Eq. (14), we obtain the hour angle of the sun at sunrise ω_{ss} or sunset ω_{sr} as follows:

$$\omega_{sr} = \cos^{-1}\left(\frac{\sin h_r - \sin\delta \sin\phi}{\cos\delta \cos\phi}\right),$$

or

$$\omega_{ss} = \cos^{-1}\left(\frac{\sin h_s - \sin\delta \sin\phi}{\cos\delta \cos\phi}\right). \quad (20)$$

Finally, substituting the values of ω_{ss} and ω_{sr} obtained from Eq. (20) and other parameters α, β, ϕ, and δ into Eq. (13), the values of R_b of each segment can be obtained.

4. Global radiation of the watershed

Monthly average daily sums of global radiation of a horizontal surface (H) in the study area are available for the period from 1965 to 1977. These data

and the cloudiness data (1951–90) from the climate station at Elkins, 24 km southeast of Parsons, were used to develop relationships predicting H at the study area for a whole study period (1951–90). The predicted values of H were then divided into diffuse and direct radiation. The relationship by Erbs et al. (1982) was used to obtain the monthly sums of diffuse radiation H_D

$$\frac{H_D}{H} = 1.317 - 3.023K_T + 3.372K_T^2 - 1.769K_T^3, \quad (21)$$

where K_T is the cloudiness index given by the ratio of global radiation at a horizontal surface (H) to extraterrestrial global radiation at a horizontal surface (H_0). The monthly average daily sums of H_0 were obtained from the following relationship (Duffie and Beckman 1974):

$$H_0 = \frac{24}{\pi} I_c \left[1 + 0.033 \cos\left(\frac{360n}{365}\right)\right] \times \left[\cos\phi \cos\delta \sin\omega_s + \pi\left(\frac{\omega_s}{180}\right) \sin\phi \sin\delta\right], \quad (22)$$

where $I_c = 1367$ W m^{-2}, is the solar constant; n is the day of the year given by Klein (1977); ϕ is geographic latitude; and δ is solar declination defined by the following relationship (Cooper 1969):

$$\delta = 23.45 \sin\left[\frac{(284 + n)360}{365}\right], \quad (23)$$

where ω_s is the sunset hour angle obtained from Eq. (12). Monthly average daily sums of direct radiation of a horizontal surface were obtained as the differences of $H - H_D$.

Shortwave radiation received at an inclined surface ($H_{\alpha\beta}$) is composed of direct and diffuse radiation and incoming radiation fluxes reflected from sites in front of the slope. For the range of slope inclination in our watershed, with the average of 14°, the isotropic approximation for sky and reflected radiation is acceptable (Belyaeva 1961). Introducing the view factor for diffuse radiation, the following relationship applies for $H_{\alpha\beta}$ (Kondratyev 1977; Belyaeva 1961):

$$H_{\alpha\beta} = (H - H_D)R_b + H_D \frac{(1 + \cos\beta)}{2} \text{VF} + R_H \frac{(1 - \cos\beta)}{2}. \quad (24)$$

The terms on the right side of the equation represent direct radiation, diffuse radiation, and reflected radiation received on a slope, respectively. The shortwave radiation reflected from a horizontal surface (R_H) was obtained from calculated global radiation for a horizontal surface using different reflectance values for forest growing season and dormant season (see below).

5. Net radiation of the watershed

The following equation was used to calculate the net radiation R_n of terrain segments in the watershed:

$$R_n = H_{\alpha\beta}(1 - r) + R_l(1 - 0.68n^2)\cos\beta, \quad (25)$$

where r is reflectance of the forest for solar radiation. The values of r are 0.17 and 0.2 for growing season and for dormant season, respectively (DeWalle and McGuire 1973; Lee and Sypolt 1974). The longwave radiation balance of the forest under cloudless sky conditions (R_l) was calculated after Berlyand (1956); n is the average monthly cloudiness in fractions of unity, and the expression ($1 - 0.68n^2$) accounts for the effect of clouds on longwave radiation balance (Budyko 1974), $\cos\beta$ accounts for the effect of slope inclination on longwave radiation exchange (Kondratyev 1977).

The equation of Berlyand for calculating R_l (W m^{-2}) has the form

$$R_l = -\delta\sigma T^4(0.39 - 0.058q^{1/2}), \quad (26)$$

where $\delta = 0.95$ is the absorptivity of the underlying surface for longwave radiation; σ is Stefan–Boltzmann constant (5.67×10^{-8} W m^{-2} K^{-4}); T (K) is the air temperature in meteorological screen; q (mm) is the vapor pressure.

6. Results

a. Description of topography

Figure 3 shows the distribution of slope inclination in the watershed. Lower sites are usually steeper than upper sites. At a given elevation, the northeast-facing slopes are usually steeper than the southeast-facing slopes. According to inclination ranges, the partial areas of the watershed expressed as percentage of its total area are $2° \leq \beta < 10°$, 25%; $10° \leq \beta < 20°$, 65%; and $20° \leq \beta \leq 29°$, 10%.

Figure 4 shows the distribution of slope azimuth in the watershed. Within defined azimuth ranges, partial areas are $0° \leq \alpha < 90°$, 23%; $90° \leq \alpha < 180°$, 62%; $180° \leq \alpha < 270°$, 13%; and $270° \leq \alpha < 360°$, 2%. With regard to the variation of azimuth and inclination, northeast-facing slopes constitute relatively large uniform sites, whereas southeast-facing slopes and those at lower elevations are characterized by a diversified structure.

b. Possible sunshine duration

The mean monthly and yearly values of the possible sunshine duration S_D were computed for all terrain segments. The mean yearly S_D of all terrain segments is 11 h with the standard deviation of 0.56 h. The mean value is 91.9% of the possible sunshine duration of a horizontal surface with unrestricted horizon. The maximum mean yearly value of S_D appears at the upper south-facing slopes and it amounts to 11.93 h. The

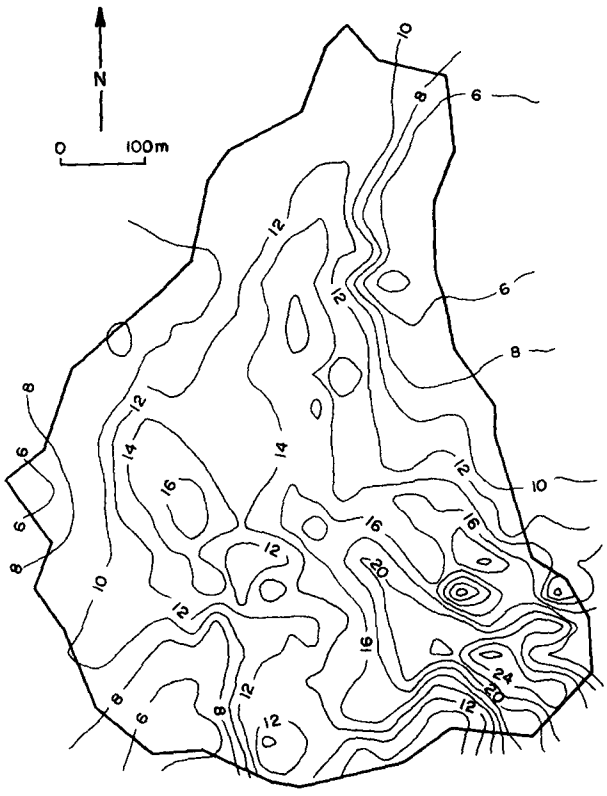

FIG. 3. Distribution of slope inclination (°) in Watershed 4.

minimum value of 9.28 h occurs at the bottom of the watershed. The relationship between the possible sunshine duration and elevation in the watershed is not statistically significant. However, the following relationship applies ($R^2 = 0.92$):

$$\text{PPS} = 1.0283 - 0.0035\beta - 0.0010\Delta\alpha, \quad \Delta\alpha \leq 90°,$$
$$\text{PPS} = 0.9035 - 0.0084\beta - 0.0009\Delta\alpha, \quad \Delta\alpha > 90°, \tag{27}$$

where PPS is the percentage of possible sunshine duration given by the ratio of possible sunshine duration of a segment (S_D) to that of a horizontal surface ($S_{D,H}$), $2° \leq \beta \leq 29°$, and $\Delta\alpha$ is the absolute value of the angle between α and the direction of the south.

The average monthly values of possible sunshine duration of terrain segments have a seasonal course. The mean July value of S_D for 432 segments is 13.5 h (93.1% of $S_{D,H}$), ranging from 12.3 h (85% of $S_{D,H}$) to 14.5 h (100% of $S_{D,H}$). The corresponding mean value for January is 8.5 h (88.6% of $S_{D,H}$), ranging from 4.7 h (49% of $S_{D,H}$) to 9.5 h (99% of $S_{D,H}$).

The seasonal variation of possible sunshine duration is smaller at south- or near south-facing slopes ($\Delta\alpha < 90°$), and greater at north- or near north-facing slopes ($\Delta\alpha > 90°$). The following relationship was obtained

$$\Delta\text{PPS}(\%) = -2.21 - 0.38\Delta\alpha + 2.886\Delta\alpha^2, \quad (R^2 = 0.80), \tag{28}$$

where ΔPPS is the difference between the PPS of segments in July and January, and $\Delta\alpha$ is in radians. The values of ΔPPS are small when $\Delta\alpha$ is less than 90°. But the values of ΔPPS increase with increasing $\Delta\alpha$ when $\Delta\alpha$ is greater than 90°.

c. *View factor*

In the case of a single slope, the value of sky view factor varies with its inclination. The VF values of a single plane ranges from 0.5 for a vertical plane to 1 for a horizontal plane. In a watershed, VF values of terrain segments are affected by the restriction of the horizon. The values of VF are generally smaller at a complex site than in a uniform area. In our study area, VF was calculated for the CG of each segment. About 75% of segments have VF greater than 0.9. The mean value of VF for 432 terrain segments is 0.91, with the maximum value 0.98 and the minimum value 0.65.

The distribution of VF in the watershed is shown in Fig. 5. The value of VF increases with the site elevation. To find the relationship between VF and site elevation, the relative elevation H_R was used

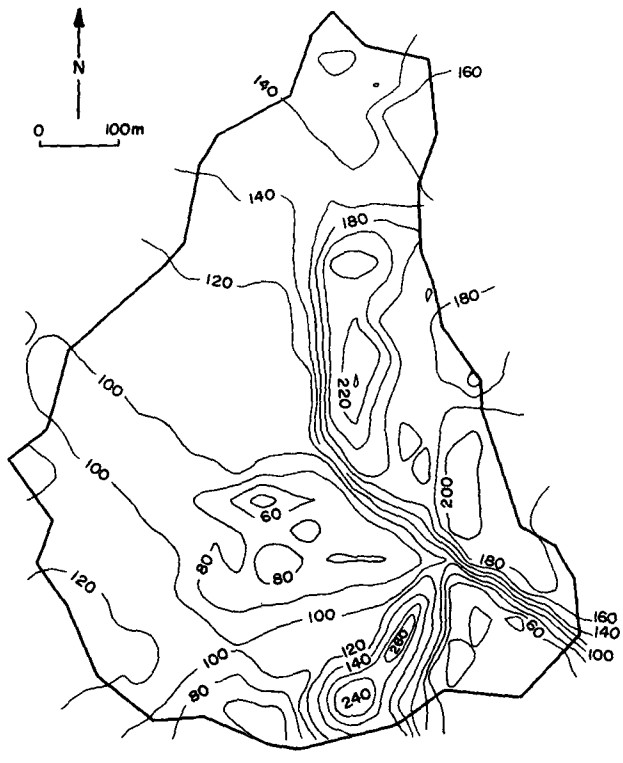

FIG. 4. Distribution of slope azimuth (°) in Watershed 4.

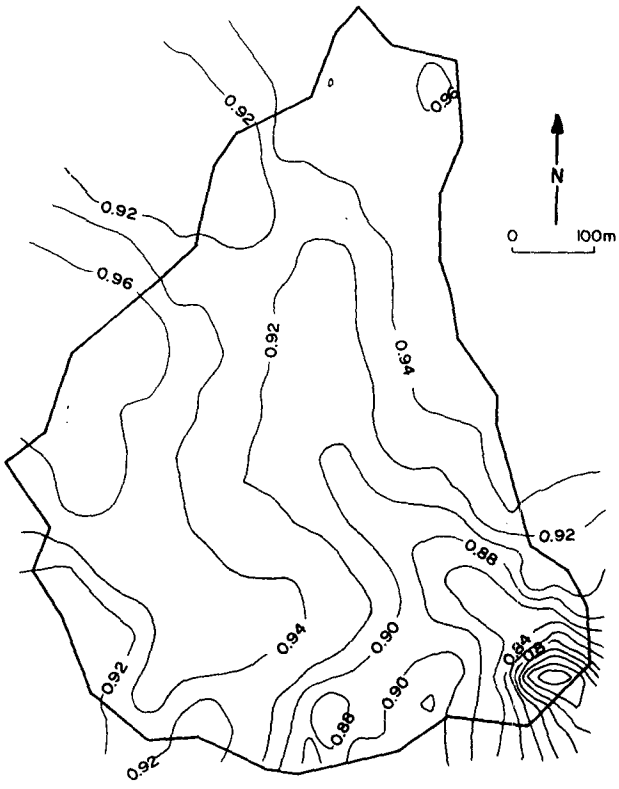

FIG. 5. Distribution of view factor in Watershed 4.

$$H_R = \frac{Z_C - Z_{\min}}{Z_{\max} - Z_{\min}}, \quad (29)$$

where Z_C is the height of the center of gravity of a segment, $Z_{\max}$ and $Z_{\min}$ are the highest and lowest elevation of the watershed, respectively. In our study area, the values of H_R range from 0.04 to 0.99. The following logarithmic relationship between the average values of VF and H_R was obtained

$$\mathrm{VF} = 0.955 + 0.07 \ln(H_R), \quad (R^2 = 0.99). \quad (30)$$

d. *Conversion factor for direct radiation*

The yearly average daily values of R_b for 432 terrain segments in our study area ranged from 0.39 to 1.42, with an average of 1.11 and standard deviation of 0.22. This means that, in the average, the watershed receives about 11% more direct solar radiation than a horizontal surface in the same area. The values of R_b are unevenly distributed in the watershed. The upper east-facing slopes have higher R_b values; while lower positions and southwest-facing slopes have relatively lower R_b values with greater variation. The upper east-facing part of the watershed receives 20%–30% more direct radiation than a horizontal surface; while the lower sites receive 10%–20% less direct radiation than a horizontal surface annually.

TABLE 2. Comparison of the conversion factor for direct radiation R_b.

Latitude	30°	30°	39.3°	39.3°
Azimuth	180°	180°	182°	180°
Inclination	30°	30°	25°	7°
	Page	Klein	Segment 35	Segment 276
January	1.61	1.66	1.82	1.26
February	1.40	1.43	1.51	1.17
March	1.18	1.20	1.25	1.09
April	0.99	1.00	1.06	1.03
May	0.89	0.87	0.95	1.00
June	0.84	0.87	0.90	0.98
July	0.85	0.84	0.92	0.99
August	0.94	0.94	1.01	1.02
September	1.09	1.12	1.17	1.07
October	1.30	1.35	1.41	1.14
November	1.53	1.60	1.71	1.23
December	1.67	1.74	1.93	1.30

The monthly values of R_b calculated by Page (1961) and by Klein (1977) are compared with those for the segments 35 and 276 at Watershed 4 (Table 2). Segment 35 was selected with the same azimuth and similar inclination as the surfaces used by Page and by Klein. Although there is a 9.3° difference in latitude, the values of R_b for segment 35 are close to those of Page's and Klein's (average relative difference is 9.2% and 6.6%, respectively). It is important to note that the seasonal variations of R_b values in Table 2 have the same pattern (i.e., high values appear in winter and low values in summer). This variation becomes weak when the segment inclination becomes gentle (segment 276). It should be noted that the values obtained by Klein and Page were for unobstructed slopes. Therefore, the difference between the values of R_b in Table 2 were also attributed to the horizon restriction.

For examining the seasonal variation of R_b at different positions in the watershed, terrain segments were arranged into four groups according to their azimuths. These groups are east ($45° \leq \alpha < 135°$), south ($135° \leq \alpha < 225°$), west ($225° \leq \alpha < 315°$), and north

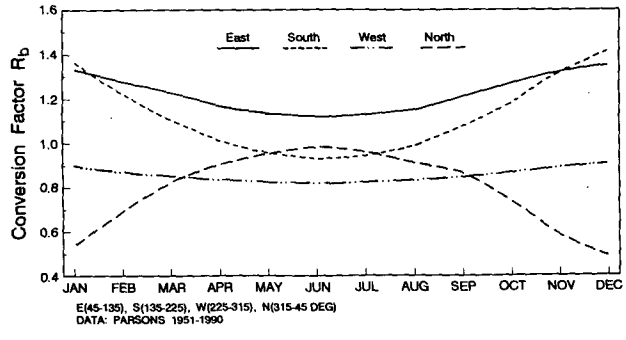

FIG. 6. Seasonal variation of the conversion factor for direct radiation at slopes with different azimuths.

($315° \leq \alpha < 45°$). The average values of R_b were calculated for each group. The results are plotted in Fig. 6. Based on Fig. 6, the seasonal variations of R_b have different patterns at differently oriented slopes. The east and south groups have higher values than west and north groups. Both the east and south groups reached their maximum values of R_b in December and the minimum values in June. But the values of R_b in the south group fluctuated more than those in the east group. Slopes in the south group have R_b values less than 1.0 (average 0.95) from May to August but greater than 1.0 in the remaining months (average 1.21). Slopes in the east group have R_b values greater than 1.0 (average 1.23) for the whole year, ranging from 1.12 to 1.36. Segments in the east group receive about 23% more direct radiation than a horizontal plane.

Slopes in the west group have relatively stable values of R_b around the year, ranging from 0.82 in June to 0.91 in December, with an average value of 0.86. This result shows that for the whole year, segments in the west group receive about 14% less direct solar radiation than a horizontal surface.

However, slopes in the north group have the greatest fluctuation of R_b in the yearly course, ranging from 0.49 in December to 0.99 in June. The value of R_b is almost equal to that of horizontal surfaces in June, but to about a half of it in December. The yearly average value of R_b is 0.79. This means that slopes in the north group receive about 21% less direct solar radiation than a horizontal plane.

The difference of average R_b between slopes in the four groups is greater in winter than in the summer. For example, the difference of R_b between the south and north groups is 0.02 in July, but it is 0.93 in December. The differences between the east and west groups is always large (average 0.37).

The above descriptions of R_b were based on Fig. 6, which reflects the topographic effects on the solar direct radiation income in this specific study area. The watershed has a southeast orientation and an average inclination of 14°. The ridgeline of the watershed tilts to the southeast. These terrain features, together with the terrain parameters of a segment, determine the specific values of R_b for a segment in the watershed at any specific time. The surrounding terrain effects on R_b of a segment are most significant in the winter season when the solar elevation is lower. To understand the different responses of slopes to solar radiation income, relationships have been obtained between solar declination δ and conversion factor R_b at different slopes (Table 3).

e. Global radiation

During the period 1951–90, the average yearly sum of global radiation, computed from the monthly average daily sums in the study area, is 4.5 GJ m^{-2} yr^{-1}. However, this energy flux varies at different terrain segments in the watershed from the minimum value of 2.8 GJ m^{-2} yr^{-1} to the maximum value of 5.3 GJ m^{-2} yr^{-1}. The distribution of the yearly sums of global radiation $H_{\alpha\beta}$ in the watershed is seen in Fig. 7. The uniformly high values of $H_{\alpha\beta}$ ($H_{\alpha\beta} > 5.0$ GJ m^{-2} yr^{-1}) are seen at the east-facing slopes in the upper part of the watershed. The southwest-facing slopes and lower sites have low values of $H_{\alpha\beta}$ ($H_{\alpha\beta} < 4.4$ GJ m^{-2} yr^{-1}). The area with the low values of $H_{\alpha\beta}$ at southwest-facing slopes may result from slope orientations because the values of R_b at southwest-facing slopes are always less than 1.0 around the year. Another area with low $H_{\alpha\beta}$ values in the lower part of the watershed is related to lower relative heights. When a segment has a low relative height, the horizon restriction will be great, which results in small solar direct and diffuse radiation income. The distributions of $H_{\alpha\beta}$ in January and July have patterns similar to those of the yearly sums in Fig. 7, but the values of $H_{\alpha\beta}$ in January are only about one-third of those in July. The shortwave radiation absorbed [$SW = H_{\alpha\beta}(1 - r)$] was also computed for terrain segments in the study area (Fu 1992).

f. Net radiation

The yearly and monthly sums of net radiation R_n of each terrain segment are closely related to its short-

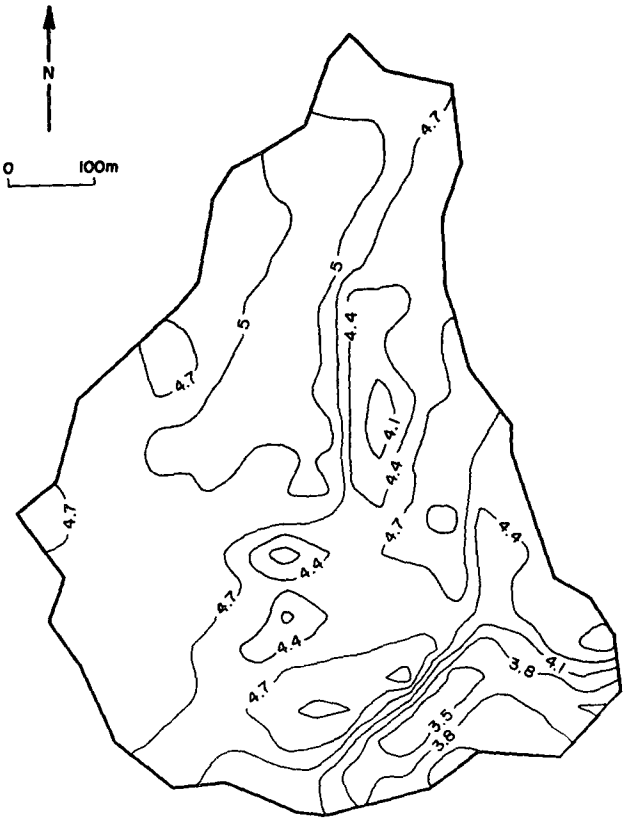

FIG. 7. Distribution of global radiation (GJ m^{-2} yr^{-1}) in Watershed 4.

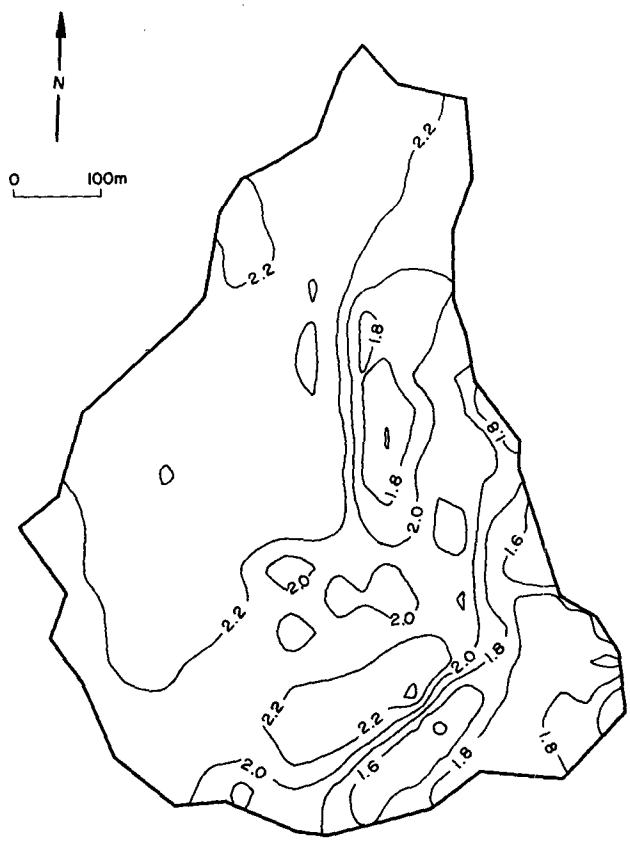

FIG. 8. Distribution of net radiation (GJ m^{-2} yr^{-1}) in Watershed 4.

wave radiation balance. For the whole watershed, the average yearly sum of R_n is 2.2 GJ m^{-2} yr^{-1} or about 50% of the average global radiation.

Spatial distribution of yearly sums of R_n is similar to that of global radiation (Fig. 8). While the distribution of R_n in July has a much similar pattern to that of the yearly sums of R_n, the distribution of R_n in January is different to some degree. The area with high R_n values is displaced to the south-facing slopes and has higher relative height than that in July. The area with negative R_n appears at the steepest northeast-facing slopes near the bottom of the watershed. This area also has the largest restriction of the horizon.

With regard to the solar radiation income, the responses of the energy balance components are different

TABLE 4. Relationships between solar declination δ (°) and average shortwave radiation absorbed SW (GJ m^{-2} $month^{-1}$) of different slopes (SW = $a + b\delta$).

	Azimuth	Inclination	a	b	R^2
East	$45° \leq \alpha < 135°$	$4° \leq \beta \leq 26°$	0.317	8.23×10^{-3}	0.98
South	$135° \leq \alpha < 225°$	$2° \leq \beta \leq 25°$	0.295	7.01×10^{-3}	0.97
West	$225° \leq \alpha < 315°$	$2° \leq \beta \leq 17°$	0.266	6.96×10^{-3}	0.98
North	$315° \leq \alpha < 45°$	$6° \leq \beta \leq 29°$	0.261	8.11×10^{-3}	0.98

in different parts of the watershed. This is due to the fact that different relationships exist between the energy balance components and the solar declination δ at different sites. The corresponding relationships for our study area are listed in Tables 3–5. These results were calculated from the grouped azimuth intervals and represent the values of the average inclination of slopes in groups.

The coefficients in the above relationships are site dependent but seasonally independent since δ is a function of time. Since solar declination δ changes continually, the relationships in Table 3 may be useful to estimate the average values of R_b for any day of the year. The relationships in Tables 4 and 5 may also be used to compute average daily values of SW and R_n by dividing their coefficients by the number of days in the month.

7. Discussion

Among the factors that affect the global radiation, the effect of reflectivity of the underlying surface on the flux density of diffuse radiation backscattered from the atmosphere and reflected from clouds toward the earth's surface has been considered rather seldom. This effect can be assessed using Ångström's formula quoted by Möller (1965). For example, when the reflectivity of a forest is 0.17 and that of a grassland is 0.25, the calculated global radiation over grassland exceeds that over forest by 7% under conditions of overcast sky and by 2.6% when the sky is partly cloudy. During the growing season, observed global radiation over forest was 11.4%–12% less than that over agricultural fields in the same area (Denmead 1968; Tajchman 1971). Global radiation over snow cover may exceed that over snow-free land by 5%–60% (Möller 1965). According to data by Kierkus and Colborne (1989), snow-covered

TABLE 3. Relationships between solar declination δ and average conversion factor for direct radiation R_b of different slopes ($R_b = a + b\delta + c\delta^2$). The conversion factor for direct radiation R_b is in fraction, the solar declination δ is in degrees.

	Azimuth	Inclination	a	b	c	R^2
East	$45° \leq \alpha < 135°$	$4° \leq \beta \leq 26°$	1.219	−0.005	3.8×10^{-5}	0.99
South	$135° \leq \alpha < 225°$	$2° \leq \beta \leq 25°$	1.089	−0.010	1.6×10^{-4}	0.99
West	$225° \leq \alpha < 315°$	$2° \leq \beta \leq 17°$	0.849	−0.002	3.0×10^{-5}	0.99
North	$315° \leq \alpha < 45°$	$6° \leq \beta \leq 29°$	0.836	0.010	-2.0×10^{-4}	0.99

TABLE 5. Relationships between solar declination δ (°) and average net radiation R_n (GJ m^{-2} month^{-1}) of different slopes ($R_n = a + b\delta$).

	Azimuth	Inclination	a	b	R^2
East	$45° \leq \alpha < 135°$	$4° \leq \beta \leq 26°$	0.184	8.06×10^{-3}	0.98
South	$135° \leq \alpha < 225°$	$2° \leq \beta \leq 25°$	0.162	6.86×10^{-3}	0.98
West	$225° \leq \alpha < 315°$	$2° \leq \beta \leq 17°$	0.131	6.79×10^{-3}	0.98
North	$315° \leq \alpha < 45°$	$6° \leq \beta \leq 29°$	0.135	7.78×10^{-3}	0.98

TABLE 6. Daily average ratios of incoming reflected radiation on inclined surfaces to radiation reflected from a horizontal surface ($r = 0.34$), after Belyaeva (1961).

Slope inclination	Slope aspect			
	North	South	East	West
10°	1.0	0.6	1.0	1.02
20°	3.2	2.4	2.9	2.7
30°	7.9	5.2	7.0	6.2
40°	14.7	10.4	13.1	13.4

ground can cause an increase in diffuse radiation by 30%–40%. The above data show that the effect of reflectivity on global radiation can be substantial. This effect can be important when global radiation data from climatic stations are applied to areas with different radiative characteristics such as surface reflectance.

In complex terrain, the geometry of diffuse radiation and reflected radiation contributes to differences in solar radiation income on slopes with different azimuth and inclination. Under such conditions, the use of isotropic approximation is limited. As a rule, in the Northern Hemisphere, south-facing slopes receive more diffuse radiation than north-facing slopes and daily sums of diffuse radiation on east-facing slopes are approximately equal to those on west-facing slopes (Schram and Thams 1967). The difference among radiation fluxes decreases when cloudiness increases, but their calculation is difficult and relevant experimental data is fragmentary and inadequate (Kondratyev 1977). Studies by Stoffel et al. (1987) and by Becker and Weingarten (1991) show that global radiation calculated from different models and diffuse radiation estimated from global radiation may differ substantially from the corresponding observed values.

Reflected radiation received at inclined surfaces is regarded as a relatively small component in the total shortwave radiation flux. However, its importance increases with slope inclination and its reflectivity. Geometry and spectral composition of shortwave reflected radiation are characterized by seasonal variation, which, for example, is related to seasonal changes of the radiative properties of land covered with vegetation (Kondratyev 1977; Sharonov 1949). The data listed in Table 6 are Belyaeva's (1961) daily average ratios of incoming reflected radiation on an inclined surface to radiation reflected from a horizontal surface ($r = 0.34$). These data show that the incoming reflected radiation increases with slope inclination, but within the inclination of 10°–40° it does not reach 15% of the radiation reflected from a horizontal surface.

8. Accuracy of the radiation data

In this particular study, global radiation data from the climate station were applied to a remote forested watershed. The distance between the climate station and the watershed is approximately 4.8 km. The elevation of the climate station is 505 m and the average elevation of the watershed is 804 m. Data on air temperature and moisture were collected at another climate station in the Fernow Forest at the elevation of 720 m. Based on measurements above similar forest stands, the reflectivity of the watershed of 0.17 for the growing season and 0.20 for the remaining part of the year was accepted. The reflectivity of the grass-covered climate station was not measured, but it may range from 0.15 to 0.25 during rainless periods (Munn 1966), and it may reach substantially higher values when the site is covered with snow. Based on the data quoted in the previous section, global radiation over the climate station may have exceeded that over the forest by 2.6%–7% during the growing season. During the winter, in the presence of snow cover at the climate station, the excess in global radiation can be much greater. It seems to be reasonable to accept that, during an average year, global radiation over the climate station exceeded that over the watershed by 5%. This effect was not taken into account in our study. Global radiation measured has an accuracy of about 5% (Munn 1966).

The relative error of net radiation ($\Delta R_n/R_n$) at the climate station can be calculated from (Pavlov 1962)

$$\frac{\Delta R_n}{R_n} = \frac{\Delta H}{H}\frac{H}{R_n} - \frac{\Delta R_r}{R_r}\frac{R_r}{R_n} + \frac{\Delta R_l}{R_l}\frac{R_l}{R_n}, \qquad (31)$$

where ΔR_n, ΔH, ΔR_r, and ΔR_l are absolute errors of net radiation, global radiation, reflected radiation, and longwave radiation balance, respectively. The relative error of R_n will be calculated for June and December of 1980. The monthly average daily sums for these two months are listed in Table 7. Accepting $\Delta H/H = \pm 5\%$,

TABLE 7. The monthly average daily sums (MJ m^{-2}) of net radiation R_n, global radiation H, reflected radiation R_r, and longwave radiation R_l at a horizontal surface in Watershed 4, Parsons, West Virginia, in June and December 1980.

	June	December
R_n	11.172	−0.403
H	18.988	4.601
R_r	3.228	0.920
R_l	−4.588	−4.084

$\Delta R_r/R_r = \pm 5\%$, and $\Delta R_l/R_l = \pm 10\%$, and assuming that all errors have the same sign, we obtain $\Delta R_n/R_n = 2.9\%$ for June and 55.7% for December. For the yearly sums, the relative error of net radiation at a horizontal surface amounts to 16%.

There are no experimental data, which could be used for direct evaluation of our results, on global radiation and net radiation on slopes. However, our values of R_b are consistent with those reported by Page (1961) and Klein (1977). The fact that yearly courses of R_b of slopes with different orientation have different patterns (Fig. 7) is of special interest for estimating spatial and seasonal variations of direct radiation in the watershed. Diffuse radiation is essentially anisotropic, however, on a yearly basis, the isotropic model provides a good first approximation of actual values (Kudish and Ianetz 1991). Kondratyev (1977) reported observed ratios of the yearly sums of global radiation on slopes to those on a horizontal surface from the Middle Urals ($\phi = 55°$–$60°$). In his opinion, these ratios can be used to estimate yearly sums of global radiation on slopes from those for a horizontal surface. Table 8 lists some of these ratios in percent for selected aspects, for which data from our watershed are available. The third line in Table 8 contains data based on our calculations. Our data are valid for the average yearly sky cover of 7.8 on a scale of 0 (clear)–10 (overcast), and for geographic latitude of 39°N. The difference between our data and those by Kondratyev, average for 10° and 20° slope inclinations, varies from 1% to 8%, with the exception of the southwest-facing slope where it reaches 14%.

In this study, diffuse radiation on a horizontal surface was obtained from global radiation using the formula by Erbs et al. (1982). A report by Becker and Weingarten (1991) shows that this formula yields underestimated values of diffuse radiation. Tajchman (1983) reported observations of diffuse radiation over the Coopers Rock Forest approximately 75 km north-northwest of Parsons for 1980. The shadow-ring correction was obtained from the relationships by Drummond (1956) and Steven and Unsworth (1980). The yearly average sky cover at Elkins, approximately 24 km south-southwest of Parsons, was 7.8 and that at Morgantown Airport, approximately 12 km south-southwest of Coopers Rock Forest, was 6.9; this difference was similar throughout the year. For 1980, the computed diffuse radiation for Parsons was 18.7% lower than the observed diffuse radiation at Coopers Rock Forest; for the period May–October the difference was 7.3%. This comparison is in agreement with results reported by Becker and Weingarten (1991).

For assessing the accuracy of the yearly sum of $H_{\alpha\beta}$, we assumed that the computed H_D values are underestimated by 10%. Since direct radiation was obtained as $(H - H_D)R_b$, the error of H_D does not substantially affect $H_{\alpha\beta}$. The relative error of $H_{\alpha\beta}$ was calculated for one south-facing segment ($\beta = 14°$) and one north-facing segment ($\beta = 13°$). Using data for 1980, we obtained −10% for the relative error of direct radiation, +10% for that of diffuse radiation, and we assumed that the relative error of the incoming reflected radiation was 10%. The relative error of the yearly sum of $H_{\alpha\beta}$ at the south-facing slope equals to 6.5% and that for the north-facing slope equals to 8.0%. The relative error of net radiation at the south-facing slope is 5.5% and 6.9% at the north-facing slope. The difference in longwave radiation exchange related to the difference in elevation between the climate station (720 m) and the watershed (804 m) and the longwave radiation exchange among slopes were assessed and they appear to be substantially less than 1% of H.

TABLE 8. Ratios in percentage of the yearly sums of global radiation on slopes to those on a horizontal surface. Data in lines 1 and 2 are from Middle Urals (55°–60°N, according to Kondratyev (1977). Data in line 3 are from Watershed 4 (39.3°N), Parsons, West Virginia.

Slope inclination	Aspect					
	North	Northeast	East	South	Southeast	Southwest
10°	91	94	100	107	105	104
20°	83	88	100	113	109	108
13°–15°	79	86	102	105	108	92

9. Conclusions

1) Slope parameters and surrounding terrain features have significant influences on solar radiation income and energy balance of a mountainous area. The energy exchange in a remote watershed can be studied by examining the temporal and spatial distributions of possible sunshine duration, view factor, and conversion factor for direct solar radiation in the watershed. Meteorological data from nearby stations can then be used in estimation of uneven distributed solar energy in the watershed.

2) In this study, the sunshine duration and the conversion factor, which determine the direct radiation income, are mainly affected by the inclination and azimuth of the segment, although the effects of the surrounding terrain exist. The view factor, which determines diffuse radiation income, is closely related to relative elevation from the valley floor. However, the terrain effects on solar radiation become more significant on steeper, north-facing slopes and at lower sites in the winter season. In Watershed 4, the lower southwest-facing slopes are also the areas with lower solar radiation income because of the southeast orientation of the watershed.

3) The approach of using a three-dimensional coordinate system for analyzing topography and energy and water balances of a forested watershed is effective, economic, and has its advantages in estimating solar energy income in complex mountainous areas. It is

applicable to describe the topographic parameters and the energy exchange in remote watersheds.

Acknowledgments. Thanks are due to Prof. Charles Yuill, Resource Management, West Virginia University, for his assistance in digitizing the topographic data. Mrs. Gloria Nestor was responsible for preparing the diagrams.

This study was supported by McIntire–Stennis funds (P. L. 87-788) and approved by the Director of West Virginia Agricultural and Forestry Experiment Station as Scientific Paper 2376.

REFERENCES

Becker, P., and D. S. Weingarten, 1991: A comparison of several models for separating direct and diffuse components of solar irradiation. *Agric. For. Meteor.*, **53**, 347–353.

Belyaeva, I. P., 1961: Potoki otrazhennoj i resseyannoj radiatsii na sklony. *Tr. Gl. Geofiz. Obs.*, **107**, 105–111.

Berlyand, M. E., 1956: *Predskazanie i Regulirovanie Teplovogo Rezhima Prizemnogo Sloya Atmosfery.* Gidromet. Izdat., Leningrad, 435 pp.

Budyko, M. I., 1974: *Climate and Life.* Academic Press, 508 pp.

Burrough, P. A., 1986: *Principles of Geographical Information System for Land Resources Assessment.* Oxford University Press, 193 pp.

Cooper, P. I., 1969: The absorption of solar radiation in solar stills. *Sol. Energy*, **12**, 333–346.

Denmead, O. T., 1968: Evapotranspiration and photosynthesis in wheat and *Pinus radiata*—A study in micrometeorology. *Proc. Ecol. Soc. Aust.*, **3**, 61–69.

DeWalle, D. R., and S. G. McGuire, 1973: Albedo variations of an oak forest in Pennsylvania. *Agrir. Meteor.*, **11**, 107–113.

Drummond, A. J., 1956: On the measurement of sky radiation. *Arch. Meteor. Geophys. Bioklimatol., Ser B.*, **7**, 413–436.

Duffie, J. A., and W. A. Beckman, 1974: *Solar Energy Thermal Processes.* Wiley Interscience, 386 pp.

Erbs, D. G., S. A. Klein, and J. A. Duffie, 1982: Estimation of diffuse radiation fraction for hourly, daily and monthly-average global radiation. *Sol. Energy*, **28**, 293–304.

Fu, H., 1992: Climatic aspects of energy and water balances of a forested Appalachian watershed. M. S. thesis, Div. Forestry, West Virginia University, 140 pp.

Iqbal, M., 1983: *An Introduction to Solar Radiation.* Academic Press, 390 pp.

Kierkus, W. T., and W. G. Colborne, 1989: Diffuse solar radiation—Daily and monthly values as affected by snow cover. *Sol. Energy*, **42**, 143–147.

Klein, S. A., 1977: Calculation of monthly average insolation on tilted surfaces. *Sol. Energy*, **19**, 325–329.

——, 1981: An algorithm for calculating monthly-average radiation on inclined surfaces. *J. of Sol. Energy Sci. Eng.*, **103**, 29–33.

Kondratyev, K., 1977: Radiation regime of inclined surfaces. WMO Tech. Note 152:52.

Kudish, A. I., and A. Ianetz, 1991: Evaluation of the relative ability of 3 models, the Isotropic, Klucher and Hay, to predict the global radiation on a tiled surface in Beer-Sheva, Israel. *Energy Convers. and Manage.*, **32**, 387–394.

Lee, R., and C. R. Sypolt, 1974: Toward a biophysical evaluation of forest site potential. *For. Sci.*, **20**, 145–154.

Liu, B. Y. H., and R. C. Jordan, 1962: Daily insolation on surfaces titled towards the equator. *Trans. ASHRAE*, 526–541.

Möller, F., 1965: On the backscattering of global radiation by the sky. *Tellus*, **17** (3), 350–355.

Munn, R. E., 1966: *Descriptive Micrometeorology.* Academic Press, 245 pp.

Page, J. K., 1961: The estimation of monthly mean values of daily total short wave radiation on vertical and inclined surfaces from sunshine records for latitudes 40°N–40°S. *Proc. UN. Conf. on New Sources of Energy*, paper S 98, **4**, 378–390.

Pavlov, A. V., 1962: Raschetnyj sposob opredelenija radiatsionnogo balansa po summarnoj radiatsii i albedo. *Izv. Akad. Nauk. SSSR, Ser. Geogr.*, **6**, 94–100.

Perez, R., and R. Stewart, 1984: Real time comparisons of models estimating irradiation on sloping surface. *Proc. 1984 Annual Meeting*, Amer. Sol. Energy Soc., Anaheim, CA, ASES, 645–650.

Peuker, T. K., R. J. Fowler, J. J. Little, and D. M. Mark, 1978: The triangulated irregular network. *Proc. of the DTM Symp.* St. Louis, MO, Amer. Soc. of Photogrammetry-Amer. Congress on Survey and Mapping, 24–31.

Schram, K., and J. C. Thams, 1967: Die Kurzwellige Strahlung von Sonne and Himmel auf verschieden orientierte und geneigte Flaechen. *Arch. Meteor. Geophys. Bioklimatol.*, Ser. B, Bd 15, H. 1-2, 99–126.

Sharonov, V. V., 1949: Problemy optiki landshafta. *Vestn. Leningr. Univ.*, **5**, 3–27.

Steven, M. D., and M. H. Unsworth, 1980: Shade-ring corrections for pyranometer measurements of diffuse solar radiation from cloudless skies. *Quart. J. Roy. Meteor. Soc.*, **106**, 865–872.

Stoffel, T. L., E. L. Maxwell, R. E. Bird, and D. R. Myers, 1987: Solar irradiance on vertical surfaces. *Passive Sol. J.*, **4**(2), 187–210.

Tajchman, S. J., 1971: Evapotranspiration and energy balances of forest and field. *Water Resour. Res.*, **7**(3), 511–523.

——, 1975: On calculating the horizon limitation and the short wave radiation income for a mountainous area. *Proc. of the 13th Int. Meeting on Alpine Meteorology*, Saint-Vincent, 174–180.

——, 1983: Solar radiation climate of a forested catchment. Forestry Notes. Agric. and For. Experim. Station, West Virginia Uniersity, No. 10, 9–10.